

FAST ALGORITHMS FOR ADAPTIVE FREE-KNOT SPLINE APPROXIMATION USING NON-UNIFORM BIORTHOGONAL SPLINE WAVELETS *

KAI BITTNER^{†‡} AND HANS GEORG BRACHTENDORF^{†§}

Abstract. New algorithms for fast wavelet transforms with biorthogonal spline wavelets on nonuniform grids are presented. In contrary to classical wavelet transforms, the algorithms are not based on filter coefficients, but on algorithms for B-spline expansions (differentiation, Oslo algorithm, etc.). Due to inherent properties of the spline wavelets, the algorithm can be modified for spline grid refinement or coarsening. The performance of the algorithms is demonstrated by numerical tests of the adaptive spline methods in circuit simulation.

Key words. Splines, spline wavelets, free knot spline approximation

AMS subject classifications. 65D07, 41A15, 65T60, 42C40

1. Introduction. Since the dawn of wavelet theory spline wavelets have been always of particular interest. This includes orthogonal spline wavelets [3, 35], semi-orthogonal spline wavelets [16, 17] as well as biorthogonal wavelets [19]. An exceptional property of spline wavelets is that they possess an explicit representation (in terms of piecewise polynomials), while most other wavelets of interest are only described by their two-scale relation. This permits extra flexibility, e.g. for the construction of wavelets on the interval [15, 21] or the evaluation of non-linear mappings of wavelet expansions [11, 18, 24].

The wavelet constructions above are based on equidistant spline knots. However, since a spline can be defined for any given grid, it arises the question if spline wavelet constructions on nonuniform grids are possible. There have been several publications on semi-orthogonal spline wavelets on non-uniform grids (see e.g. [14, 33, 37]). Although these wavelets do not have a sparse decomposition relation, there are fast algorithms, which solve a banded linear system involving the reconstruction coefficients (cf. [41]). However, in some cases finite decomposition relations as they appear for biorthogonal spline wavelets [19, 21] may be of interest. A constructive proof of the existence of such spline wavelets in the nonuniform setting was given in [22], based on results of banded matrices with banded inverses. However, no algorithms based on this approach are provided.

In [4] we have given sufficient and necessary conditions for the existence of finite reconstruction and decomposition relations. However, an algorithm based on this relation requires the computation of many coefficients, which is time and memory consuming. Thus, we have developed a direct approach based on known properties of spline functions. Here we will present algorithms for the fast wavelet transform for non-uniform spline wavelets, which represent a generalization of the biorthogonal spline wavelets from [19]. By a small modification we obtain also an algorithm for adaptive knot removal, which permits to reduce the size of a spline representation with the approximation error under control. Furthermore, we introduce an adaptive spline approximation method with adaptive grid refinement. These algorithms were

*This work has been partly supported by the ENIAC research project ARTEMOS under grant 829397 and the FWF under grant P22549.

[†]University of Applied Sciences Upper Austria, Softwarepark 11, A-4232 Hagenberg, Austria

[‡]Kai.Bittner@fh-hagenberg.at

[§]Hans-Georg.Brachtendorf@fh-hagenberg.at

used to develop a wavelet based adaptive method for circuit simulation [7–10]. In this context the use of wavelets on non-uniform grids appears to be much more suitable than a method based on uniform wavelets. Here we will give a complete description of the wavelet transforms.

In §2 we will recall basic properties of spline functions and B-splines, which are important for our approach. The wavelet bases for non-uniform grids will be introduced in §3. The fast decomposition and reconstruction algorithm is described in §4. §5 discusses several modifications of our approach. In particular the restriction to an interval and to periodic functions is of practical interest. Based on the fast decomposition algorithm, methods for grid coarsening and refinement are introduced in §6. The performance of this grid adaptation is demonstrated by a numerical test on a multirate circuit simulation problem in §7.

2. Spline functions and B-splines. In this section we establish our notation and recall basic facts and algorithms for splines, which are needed for our new algorithms. For a detailed introduction to splines we refer to [25, 42].

For a given knot sequence $\mathcal{T} = (t_i)_{i \in \mathbb{Z}}$ satisfying

$$t_i < t_{i+1}, \quad (2.1)$$

the *spline space* of order m is defined as

$$S_{m,\mathcal{T}} = \left\{ f \in C^{m-2}(\mathbb{R}) : f|_{(t_i, t_{i+1}]} \in \Pi_{m-1} \right\}.$$

Here, Π_{m-1} denotes the space of polynomials of degree less than m . It is also possible to consider multiple knots, i.e., $t_i = \dots = t_{i+\ell}$. In this case the spline functions possess only $m - 2 - \ell$ continuous derivatives in t_i . Since we will need multiple knots for spline wavelets on a closed interval we include the corresponding modifications in the sequel.

A basis for $S_{m,\mathcal{T}}$ is given by the B-splines $N_{m,k} = N_{m,k}^{\mathcal{T}}$, $k \in \mathbb{Z}$, which are the uniquely determined spline functions of minimal support $[t_k, t_{k+m}]$ satisfying $\sum_{k \in \mathbb{Z}} N_{m,k}(1) \equiv 1$.

Values of a spline function s can be computed from the coefficients c_k of its B-spline expansion $s = \sum_{k \in \mathbb{Z}} c_k N_{m,k}$ by the de Boor algorithm. For $t \in (t_k, t_{k+1}]$ the value $s(t) = c_k^{(m-1)}$ is computed by the recursion

$$c_k^{(\ell)} = \begin{cases} c_k, & \text{if } \ell = 0, \\ \frac{(t - t_k) c_k^{(\ell-1)} + (t_{k+m-\ell} - t) c_{k-1}^{(\ell-1)}}{t_{k+m-\ell} - t_k}, & \text{if } t \in (t_k, t_{k+m-\ell}], \\ 0 & \text{otherwise.} \end{cases} \quad (2.2)$$

Furthermore, derivatives of the B-splines are given by

$$N'_{m,k}(t) = (m-1) \left(\frac{N_{m-1,k}(t)}{t_{k+m-1} - t_k} - \frac{N_{m-1,k+1}(t)}{t_{k+m} - t_{k+1}} \right). \quad (2.3)$$

Therefore the derivative of the spline function $s = \sum_{k=0}^n c_k N_{m,k}$ is given as $s' = \sum_{k=0}^n c'_k N_{m-1,k}$, with

$$c'_k = \begin{cases} (m-1) \frac{c_k - c_{k-1}}{t_{k+m-1} - t_k} & \text{if } t_k < t_{k+m-1}, \\ 0 & \text{otherwise.} \end{cases} \quad (2.4)$$

For our wavelet construction we have to deal with nested spline spaces. Obviously, the spline space $S_{m,\Delta}$ is contained in $S_{m,\mathcal{T}}$ if and only if $\Delta = (\tau_k)_{k \in \mathbb{Z}} \subset \mathcal{T} = (t_\ell)_{\ell \in \mathbb{Z}}$, i.e., \mathcal{T} is a *refinement* of Δ .

Any spline $s = \sum_{k=1}^N c_k^\Delta N_{m,k}^\Delta \in S_{m,\Delta}$ is also contained in $S_{m,\mathcal{T}}$ and has the B-spline representation $s = \sum_{k=1}^n c_k^\mathcal{T} N_{m,k}^\mathcal{T}$ with respect to the finer grid. The coefficients $c_k^\mathcal{T}$ can be computed from the c_k^Δ by the Oslo algorithm [20, 36] as follows. For $t_i \in (\tau_j, \tau_{j+1}]$ the coefficient $c_i^\mathcal{T} = c_{j,i}^{(m-1)}$ is determined by the recursion

$$c_{j,i}^{(k)} = \begin{cases} c_j^\Delta, & \text{if } k = 0, \\ \frac{(t_{i+m-k} - \tau_j)c_{j,i}^{(k-1)} + (\tau_{j+m-k} - t_{i+m-k})c_{j-1,i}^{(k-1)}}{\tau_{j+m-k} - \tau_j}, & \text{if } t_{i+m-k} \in (\tau_j, \tau_{j+m-k}], \\ 0 & \text{otherwise.} \end{cases} \quad (2.5)$$

The insertion of a single knot, i.e., $\mathcal{T} = (\tau_1, \dots, \tau_{j-1}, t, \tau_j, \dots, \tau_N)$ can also be done by Boehm's knot insertion algorithm [12]

$$c_i^\mathcal{T} = \begin{cases} c_i^\Delta, & \text{if } i \leq j - m \\ \frac{(\tau_{i+m} - t)c_{i-1}^\Delta + (t - \tau_i)c_i^\Delta}{\tau_{i+m} - \tau_i}, & \text{if } j - m < i < j, \\ c_{i-1}^\Delta, & \text{if } i \geq j. \end{cases} \quad (2.6)$$

3. A class of spline wavelets for non-uniform grids. Spline wavelets on nonuniform grids with finite decomposition and reconstruction sequences have been investigated in [4]. To have an efficient and readable algorithm we consider a subclass of these spline wavelets, which can be considered as a generalization of spline wavelets for uniform grids [19], as pointed out in [5]. We will illustrate possible generalizations after establishing our fast algorithm.

We start from a lattice of nested knot sets $\mathcal{T}^j = (t_i^j)_{i \in \mathbb{Z}}$ satisfying $t_i^j < t_{i+1}^j$, where either $t_i^j = t_{2i}^{j+1}$ or

$$t_i^j = \begin{cases} t_{n_1^j+i}^{j+1}, & \text{if } i < n_1^j, \\ t_{2i}^{j+1}, & \text{if } i = n_1^j, \dots, n_2^j \\ t_{n_2^j+i}^{j+1}, & \text{if } i > n_2^j. \end{cases} \quad (3.1)$$

The classical setting would be $n_1^j = -\infty$ and $n_2^j = \infty$, while finite values for n_1^j and n_2^j yield a local refinement of \mathcal{T}^j , where additional knots are only inserted in the interval $[t_{n_1^j}^0, t_{n_2^j}^0]$. Obviously, the corresponding spline spaces $V_j := S_{m,\mathcal{T}^j}$ are nested, i.e., $V_j \subset V_{j+1}$. Therefore, we consider $\{V_j : j \in \mathbb{Z}\}$ as generalized Multiresolution Analysis with scaling functions

$$\varphi_k^j := N_{m,k}^{\mathcal{T}^j}.$$

Then, we define wavelets as

$$\psi_k^j(t) := \alpha_k^j \frac{d^{\tilde{m}}}{dt^{\tilde{m}}} N_{m+\tilde{m},0}^{\Xi_k^j}(t), \quad k = n_1^j, \dots, n_2^j - 1. \quad (3.2)$$

where

$$\Xi_k^j = (\xi_{k,\ell}^j)_{\ell=0}^{m+\tilde{m}} := (t_{k+1-\ell_1}^j, t_{k+2-\ell_1}^j, \dots, t_k^j, t_{2k+1}^{j+1}, t_{k+1}^j, \dots, t_{k-1+\ell_2}^j, t_{k+\ell_2}^j) \quad (3.3)$$

with $\ell_1 = \lfloor \frac{m+\tilde{m}}{2} \rfloor$, $\ell_2 = \lceil \frac{m+\tilde{m}}{2} \rceil$. Note, that t_{2k+1}^{j+1} is the only knot in Ξ_k^j which is not contained in \mathcal{T}^j . Thus, each wavelet represents the contribution of one and only one knot from $\mathcal{T}^{j+1} \setminus \mathcal{T}^j$. This property will be a key ingredient for our fast wavelet transform algorithm. The term α_k^j in (3.2) denotes a normalization factor, which can e.g. be chosen according to a particular function space. In §6.1 (Eq. (6.3) and enclosing text) we give an example how this factor can be chosen in an application.

As demonstrated in [4, 5], we have the following properties:

- (i) $\psi_k^j \in V_{j+1}$ and $\psi_k^j \notin V_j$,
- (ii) Compact support: $\text{supp } \psi_k^j = [t_{k+1-\ell_1}^j, t_{k+\ell_2}^j]$,
- (iii) \tilde{m} Vanishing moments: $\int_{\mathbb{R}} \psi_k^j(t) t^\ell dt = 0$, $\ell = 0, \dots, \tilde{m} - 1$,
- (iv) Finite reconstruction relations:

$$\varphi_k^j = \sum_{\ell=2k}^{2k+m} \alpha_{k,\ell}^j \varphi_\ell^{j+1} \quad \text{and} \quad \psi_k^j = \sum_{\ell=2(k+1-\ell_1)}^{2(k+\ell_2)-m} b_{k,\ell}^j \varphi_\ell^{j+1}, \quad (3.4)$$

- (v) Finite decomposition relations:

$$\varphi_k^{j+1} = \sum_{\ell \in \mathcal{I}_k^j} c_{k,\ell}^j \varphi_\ell^j + \sum_{\ell \in \mathcal{J}_k^j} d_{k,\ell}^j \psi_\ell^j \quad \#\mathcal{I}_k^j < \tilde{m} + \lceil \frac{m}{2} \rceil, \quad \#\mathcal{J}_k^j < \lceil \frac{m}{2} \rceil, \quad (3.5)$$

(vi) Generalization of existing wavelets: For uniform dyadic grids, i.e. if $t_k^j = 2^{-j}k$, and for $m + \tilde{m}$ even, the wavelets coincide with the biorthogonal spline wavelets introduced in [19]. These wavelets are widely used in Numerical Analysis, since there exist well understood generalizations to intervals [4, 21, 38] and domains [23, 34] and since spline wavelets are also optimal for the handling of non-linear problems [1, 11, 18, 24].

Most definitions of wavelet systems include also a stability condition (e.g. orthonormal basis, Riesz basis), which ensures that small disturbances of the coefficients cause only small deviations of the spline function and vice versa. While proofs of Riesz stability exist in the uniform case, similar results are much harder to obtain for the nonuniform case. While there is some numerical evidence that the wavelet transform are stable, the theoretical foundation will be the target of future research.

The relations (3.4) and (3.5) permit a fast wavelet transform. The wavelet transforms (decomposition and reconstruction) are a change of basis between $\{\varphi_k^{j+1}\}$ and $\{\varphi_k^j\} \cup \{\psi_k^j\}$, which can be done fast due to the finiteness of the sums. To perform these transforms we need to know the coefficients $a_{k,\ell}^j$, $b_{k,\ell}^j$, $c_{k,\ell}^j$, and $d_{k,\ell}^j$. The computation of these coefficients is possible but costly in computation time and storage. Therefore, we propose here a direct way based on the proofs in [4, 5], which is more practicable.

4. Algorithms for the fast wavelet transform.

4.1. Fast wavelet decomposition. The wavelet decomposition algorithm, also called wavelet analysis or just fast wavelet transform, computes from given spline coefficients c_k^{j+1} the coarse scale spline coefficients c_k^j and the corresponding wavelet coefficients d_k^j satisfying

$$s_{j+1} := \sum_{k \in \mathbb{Z}} c_k^{j+1} \varphi_k^{j+1} = \sum_{k \in \mathbb{Z}} c_k^j \varphi_k^j + d_k^j \psi_k^j. \quad (4.1)$$

In the sequel we assume without loss of generality that $j = 0$. Furthermore, we assume that s_1 is compactly supported in $[t_0^0, t_n^0]$ such that all sums are finite, which is reasonable from the computational point of view. Obviously, we can then assume that in (3.1) $n_1^0 = 0$ and $n_2^0 = n$.

Computation of the wavelet coefficients. Any spline can be written in its truncated power representation

$$s_1(t) = \sum_{k \in \mathbb{Z}} a_k (t - t_k^1)_+^{m-1}, \quad (4.2)$$

where $(t)_+^j = \chi_{(0, \infty)}(t) t^j$ are the truncated powers. Due to (3.2) and (3.3), the wavelets have the representation

$$\psi_k^0(t) = \sigma_k(t) + \gamma_k (t - t_{2k+1}^1)_+^{m-1}, \quad (4.3)$$

where $\gamma_k \in \mathbb{R}$ and σ_k is a suitable spline from V_0 . Applying (4.3) to (4.1) we obtain

$$s_1(t) = s_0(t) + \sum_k d_k^0 \sigma_k(t) + \sum_k d_k^0 \gamma_k (t - t_{2k+1}^1)_+^{m-1} \quad (4.4)$$

Obviously $\tilde{\sigma} := s_0 + \sum_k d_k \sigma_k$ is a spline from V_0 , while $\gamma_k (t - t_{2k+1}^1)_+^{m-1}$ is the contribution from the ‘new’ knot t_{2k+1}^1 . By comparison of coefficients in (4.2) and (4.4) we conclude that

$$\tilde{\sigma}(t) = \sum_{k \in \mathbb{Z}} a_{2k} (t - t_{2k}^1)_+^{m-1}$$

and

$$d_k^0 = \frac{a_{2k+1}}{\gamma_k},$$

i.e., if we know a_{2k+1} and γ_k we can easily compute the wavelet coefficient d_k^0 .

To determine the coefficients of the truncated power representation we use the following fact. Obviously the $(m-1)$ -th derivative of s_1 is given as

$$s_1^{(m-1)} = (m-1)! \sum_{k \in \mathbb{Z}} a_k \chi_{(t_k^1, \infty)}.$$

On the other hand, applying the differentiation rule (2.4) we can compute coefficients β_k from the known spline coefficients c_k^1 such that

$$s_1^{(m-1)} = \sum_{k \in \mathbb{Z}} \beta_k N_{1,k}^{\mathcal{T}^1}.$$

Since $N_{1,k}^{\mathcal{T}^1} = \chi_{(t_k^1, t_{k+1}^1]}$ we conclude immediately that

$$a_k = \frac{\beta_k - \beta_{k-1}}{(m-1)!}. \quad (4.5)$$

Analogously to a_{2k+1} we determine γ_k from the $(m+\tilde{m}-1)$ -th derivative of $\alpha_k^j N_{m+\tilde{m},0}^{\Xi_k^0}$, which is by (3.2) the $(m-1)$ -th derivative of ψ_k^1 , i.e.,

$$\gamma_k = \frac{\rho_{k,\ell_1} - \rho_{k,\ell_1-1}}{(m-1)!}, \quad (4.6)$$

where the $\rho_{k,\ell}$ are given by

$$\alpha_k^j \frac{d^{m+\tilde{m}-1}}{dt^{m+\tilde{m}-1}} N_{m+\tilde{m},0}^{\Xi_k^0}(t) = \sum_{\ell=0}^{m+\tilde{m}-1} \rho_{k,\ell} N_{1,\ell}^{\Xi_k^0}(t).$$

Coarse scale approximation. Furthermore, one has to compute the coarse scale approximation

$$s_0 = \sum_{k \in \mathbb{Z}} c_k^0 \varphi_k^0 = s_1 - \sum_{k \in \mathbb{Z}} d_k^0 \psi_k^0.$$

In order to subtract the wavelets from the spline s_1 we need the representation of ψ_k^0 in terms of the φ_k^1 . Applying the differentiation formula (2.4) \tilde{m} times to $\alpha_k N_{m+\tilde{m},0}^{\Xi_k^0}$ (cf. 3.2) will yield the representation¹

$$\psi_k^0 = \sum_{\ell=0}^{\tilde{m}} u_{k,\ell} N_{m,\ell}^{\Xi_k^0} \quad (4.7)$$

in terms of B-splines over $\Xi_k^0 \subset \mathcal{T}^1$. The required representation

$$\psi_k^0 = \sum_{\ell \in \mathbb{Z}} b_{k,\ell} \underbrace{N_{m,\ell}^{\mathcal{T}^1}}_{\varphi_\ell^1} \quad (4.8)$$

is then obtained by the Oslo algorithm (2.5). Due to the compact support of ψ_k^1 there are only $2\tilde{m} + m - 2$ non-vanishing coefficients $b_{k,\ell}$ for each k . Now, we are able to subtract the wavelet representation from s_1 and obtain

$$s_0 = \sum_{k \in \mathbb{Z}} \tilde{c}_k \varphi_k^1$$

with

$$\tilde{c}_k = c_k^0 - \sum_{\ell=0}^{n-1} b_{\ell,k} d_\ell^0. \quad (4.9)$$

Knot removal. The above computations yield a representation of $s_0 \in V_0$ in terms of the B-splines $\varphi_1 = N_{m,k}^{\mathcal{T}^1}$. Since we are looking for a representation in terms of the $\varphi_0 = N_{m,k}^{\mathcal{T}^0}$, we need a method to ‘remove’ the knots t_{2k+1}^0 . This can be done using an inversion of Boehm’s algorithm (2.6) (cf. [27]). We will remove the knots step by step. This means that in the k -th step we have to replace the representation $s_1 = \sum_{\ell} p_\ell^k N_{m,\ell}^{\Theta_k}$ by $s_1 = \sum_{\ell} p_\ell^{k+1} N_{m,\ell}^{\Theta_{k+1}}$, where $\Theta_k = (\theta_i^k)_{i \in \mathbb{Z}}$ with

$$\theta_{k+i}^k = \begin{cases} t_{k+i}^0, & \text{if } i \leq 0 \\ t_{2k+i}^1, & \text{if } i > 0, \end{cases} \quad (4.10)$$

i.e., $\mathcal{T}^1 = \Theta_0$ and $\mathcal{T}^0 = \Theta_n$. Starting from $p_\ell^0 = \tilde{c}_\ell$ we obtain the required coefficients as $c_\ell^1 = p_\ell^n$.

¹This can be done as part of the computation of γ_k above.

Following Boehm's algorithm in (2.6) the coefficients are related by

$$p_i^k = \begin{cases} p_i^{k+1}, & \text{if } i \leq k - m \\ \frac{(\theta_{i+m}^{k+1} - t_{2k+1})p_{i-1}^{k+1} + (t_{2k+1} - \theta_i^{k+1})p_i^{k+1}}{\theta_{i+m}^{k+1} - \theta_i^{k+1}}, & \text{if } k - m < i < k, \\ p_{i-1}^{k+1}, & \text{if } i \geq k. \end{cases}$$

Thus, given p_i^k we obtain p_i^{k+1} by $p_i^{k+1} = p_i^k$, $i \leq k - m$, $p_i^{k+1} = p_{i+1}^k$, $i \geq k - 1$, and either

$$p_i^{k+1} = \frac{(\theta_{i+m}^{k+1} - \theta_i^{k+1})p_i^k - (\theta_{i+m}^{k+1} - t_{2k+1})p_{i-1}^{k+1}}{t_{2k+1} - \theta_i^{k+1}} \quad (4.11)$$

or

$$p_i^{k+1} = \frac{(\theta_{i+1+m}^{k+1} - \theta_{i+1}^{k+1})p_{i+1}^k - (t_{2k+1} - \theta_{i+1}^{k+1})p_{i+1}^{k+1}}{\theta_{i+1+m}^{k+1} - t_{2k+1}} \quad (4.12)$$

for $k - m < i < k - 1$. Both recursions yield the same result, if computed in exact arithmetic, since $s_1 \in S_{m, \mathcal{T}^1}$ and $t_{2k+1} \notin \mathcal{T}^1$.

However, rounding in floating point computations may lead to different results. Numerical test show that (4.11) is numerically unstable, while (4.12) yields the expected result. This behavior can be explained by the following observation. Obviously $c_{k-m} = p_{k-m}^k$, i.e., c_{k-m} is determined after the removal of $k - 1$ knots. In (4.11) the computation of p_{k-m+1}^{k+1} involves $p_{k-m}^k = p_{k-m}^{k+1}$, which in turn depends on computations of the previous steps down to p_{1-m}^1 . Thus rounding errors of all computations can accumulate and the error may increase with k . In practice it can indeed be observed that the error exceeds the magnitude of the coefficients for moderate sized k .

On the other hand, for (4.12) the coefficient p_{k-m}^k depends only on p_i^{k-1} , $i = k - m + 1, \dots, k - 1$. Successive application of this argument yields that p_{k-m}^k depends only on p_i^{k-j} , $i = k - m + j, \dots, k - 2 + j$. Since $p_i^{k-m} = \tilde{c}_{i+k-m-1}$, $i = k, \dots, k - 2 + m$, it follows that rounding errors made until step $k - m - 1$ have no influence on result for p_{k-m}^k . Thus, the accuracy of the floating point computations does not depend on k and the computation by (4.12) is stable, which is confirmed by numerical tests.

The difference in stability is due to the fact, that we are removing the knots from 'left' to 'right' (cf. (4.10)). The recursion (4.11), which is going also from left to right starts from $p_{k-m}^{k+1} = p_{k-m}^k$, which contains the rounding error from the previous knot removal. The recursion (4.12) goes from right to left starting from $p_{k-1}^{k+1} = p_k^k$, which was not touched by previous computations.

Summing up we have the following algorithm for the wavelet decomposition.

ALGORITHM 1.

Wavelet decomposition

INPUTS: m spline order
 \tilde{m} number of vanishing moments for wavelets
 $(t_i^0)_i$ spline knot sequence
 $(c_i^1)_i$ vector of spline coefficients

OUTPUTS: $(c_i^0)_i$ vector of spline coefficients
 $(d_i^0)_i$ vector of wavelet coefficients

CODE:

1. *Wavelet coefficients and coarse scale approximation*
 - (a) Compute truncated power coefficients $(a_{2k+1})_k$ by (2.4) and (4.5)
 - (b) FOR $k = 0, \dots, n-1$ (*loop over wavelets*)
 - i. Compute coefficients $b_{\ell,k}$ for (4.8) by (2.4) and Oslo algorithm (2.5)
 - ii. Compute truncated power coefficient γ_k by (2.4) and (4.6)
 - iii. $d_k^0 = \frac{a_{2k+1}}{\gamma_k}$
 - iv. FOR $\ell = 2(k+1-\ell_1), \dots, 2(k+\ell_2) - m$

$$c_\ell^1 := c_\ell^1 - b_{k,\ell} d_k^0 \quad (\text{subtract } d_k^0 \psi_\ell^0 \text{ from } s_1)$$
2. *Knot removal*
 - (a) $p_i^0 = c_i^1, i = 0, \dots, n$
 - (b) FOR $k = 0, \dots, n-1$ (*loop over wavelet knots*)
 - Compute p_i^{k+1} by (4.12)
 - (c) $c_i^0 := p_i^n$

Obviously the number of floating point operation is bounded by Cn , with some constant depending on m and \tilde{m} , i.e., we have indeed presented a fast algorithm. However, C is considerably larger compared to the uniform case.

For equidistant knots, we have due to translation invariance that $c_{k,\ell}^j = p_{2\ell-k}$ and $d_{k,\ell}^j = q_{2\ell-k}$. Since the $m+2\tilde{m}$ non-vanishing coefficients p_ℓ and the m non-vanishing coefficients q_ℓ can be determined in advance, the well known classical algorithm based on the decomposition relation (3.5) will need $4(m+\tilde{m})n$ floating point operations.

The performance of Algo. 1 is essentially reduced by the computations in steps 1(b)i–iii, which depend only on the used wavelets, but not on the input spline. If we want to decompose several splines over the same grid, these computations are repeated again and again. To avoid this effect, we collect all splines into a vector valued function, which means that the corresponding coefficients $c_k^j, d_k^j, a_k,$ and p_i^k in the algorithm become vectors from \mathbb{R}^N . This approach avoids extra memory to store quantities as $b_{i,k}$ and γ_k , and is motivated by our applications in circuit simulation as described in §7. Counting the floating point operations for each step yields then

1(a):	$(4N+4)(m-1)n + nN$
1(b)i: (2.5)	$\frac{7}{2}(2\tilde{m}+m-1)(m-1)mn$
1(b)ii and 2(b)i (2.4):	$n + n \sum_{k=0}^{\tilde{m}+m-1} 4k = n + 2(\tilde{m}+m)(\tilde{m}+m-1)n$
1(b)iii:	n
1(b)iv:	$2(2\tilde{m}+m)nN$
2.	$(4N+3)(m-2)n$
Total:	$N(4\tilde{m}+10m-11)n$
	$+ \{m^2(3.5m+7\tilde{m}-5) + \tilde{m}(2\tilde{m}-3m-2) + 8.5m-8\}n$

Here, we have used that the computation of the $u_{k,\ell}$ in (4.7) is an intermediate result in the computation of γ_k , while the division by $(m-1)!$ in (4.5) and (4.6) can be omitted yielding the same result. Obviously, for sufficiently large N the algorithm will need two to three times as much operations as the classical wavelet transform on a grid of the same size. However, a nonuniform grid may be chosen much smaller in some cases, due to its flexibility. Thus, the use of nonuniform spline wavelets may be beneficial for suitable applications, as we will demonstrate in an example in §7.

The decomposition algorithm can be applied again to s_1 , which is decomposed in a coarser signal s_2 and details w_2 . The successive application of this approach, also known as the pyramid scheme, yields the multiscale decomposition

$$s_J = s_0 + \sum_{j=0}^{J-1} \sum_{k \in \mathbb{Z}} d_k^j \psi_k^j. \quad (4.13)$$

4.2. Fast wavelet reconstruction. In order to transform a wavelet representation into the corresponding B-spline representation, we have to solve the following reverse problem. Given coefficients c_k^0 and d_k^0 , we have to compute coefficients c_k^1 which satisfy (4.1). In fact this problem can be solved immediately by the Oslo algorithm yielding $s_0 = \sum_{k \in \mathbb{Z}} \tilde{c}_k^1 \varphi_k^1$ and $\psi_k^1 = \sum_{\ell \in \mathbb{Z}} b_{k,\ell} \varphi_\ell^1$. Then we obtain the required coefficients immediately as $c_k^1 = \tilde{c}_k^1 + \sum_{\ell \in \mathbb{Z}} b_{\ell,k} d_\ell^0$.

ALGORITHM 2.

Wavelet reconstruction

INPUTS: m spline order
 \tilde{m} number of vanishing moments for wavelets
 $(t_i^0)_i$ spline knot sequence
 $(c_i^0)_i$ vector of spline coefficients
 $(d_i^0)_i$ vector of wavelet coefficients
OUTPUT: $(c_i^1)_i$ vector of spline coefficients
CODE:
1. Compute $(\tilde{c}_i^1)_i$ by the Oslo algorithm (2.5)
2. $(c_i^1)_i = (\tilde{c}_i^1)_i$
3. FOR $k = 0, \dots, n-1$ (loop over wavelets)
(a) Compute coefficients $b_{k,\ell}$ in (4.8) by successive differentiation (2.4) and Oslo algorithm (2.5)
(b) FOR $\ell = 2(k+1-\ell_1), \dots, 2(k+\ell_2)-m$
 $c_\ell^1 := c_\ell^1 + b_{k,\ell} d_k^0$ (Add $d_\ell^0 \psi_\ell^0$ to s_1)

Analogously to Algo. 1 we determine the computational cost of Algo. 2 for vector valued input

1:	$(4N+3)m(m-1)n$
3(a) (2.4):	$n \sum_{k=0}^{\tilde{m}} 4k = 2\tilde{m}(\tilde{m}+1)n$
3(a) (2.5):	$\frac{7}{2}(2\tilde{m}+m-1)(m-1)m n$
3(b):	$2(2\tilde{m}+m)n N$
Total:	$N(4\tilde{m}+m(4m-2))n$
	$+ \{m^2(3.5m+7\tilde{m}-4) + \tilde{m}(2\tilde{m}-7m+6) + 2.5m\}n$

Again the algorithm is more costly than the classical algorithm for a uniform grid with $4N(m + \tilde{m})n$ operations. However, if a much smaller, adapted grid can be used a nonuniform grid is of advantage. Another question is how a suitable nonuniform grid can be determined. Questions like this have lead to the investigation of non-linear approximation methods. For a survey we refer the reader to [26]. In Sect 6 we present methods to determine an optimal adaptive grid using modifications of our wavelet algorithms.

5. Modifications of the wavelet definition.

5.1. Spline wavelets on the interval. In many cases, one needs spline representation on a compact interval $[a, b]$. It is reasonable to choose the end points as spline knots, i.e., $t_0 = a$ and $t_n = b$. and define the spline space

$$S_{m,\mathcal{T}}([a, b]) := \left\{ s|_{[a,b]} : s \in S_{m,\mathcal{T}} \right\},$$

i.e., the restriction of $S_{m,\mathcal{T}}$ onto $[a, b]$. Obviously,

$$S_{m,\mathcal{T}}([a, b]) := \text{span} \left\{ N_{m,k}|_{[a,b]} : k = 1 - m, \dots, n - 1 \right\},$$

and only the knots $t_{1-m}, \dots, t_{n+m-1}$ play a role for the spline space and the B-splines.

The spline space $S_{m,\mathcal{T}}([a, b])$ does not depend on the particular choice of the outer knots t_{-i} and t_{n+i} , $i > 0$, but they influence the B-Splines at the boundary. For stability reasons and simplicity one chooses multiple knots at the boundary, i.e., $t_{-i} = t_0 = a$ and $t_{n+i} = t_n = b$, $i > 0$.

Wavelets can be defined in principle as before with nested knot sequences $\mathcal{T}^j = (t_k^j)_{k \in \mathbb{Z}}$, $j \in \mathbb{N}_0$,

$$t_k^j = \begin{cases} a, & \text{if } k \leq 0, \\ b, & \text{if } k \geq n_j, \\ t_{2k}^{j+1} & \text{otherwise,} \end{cases}$$

where $n_j = \lceil n_{j+1}/2 \rceil$. However, to ensure \tilde{m} vanishing moments we need all derivatives of $N_{m+\tilde{m},0}^{\Xi_k^j}$ to vanish at the boundaries. Therefore, we modify the definition of Ξ_k^j in (3.3) to

$$\Xi_k^j := \begin{cases} (t_{2-m}^j, t_{3-m}^j, \dots, t_k^j, t_{2k+1}^{j+1}, t_{k+1}^j, \dots, t_{m+1}^j), & \text{if } 0 \leq k < 1 - m + \ell_1 \\ (t_{n_j - \tilde{m} - 1}^j, \dots, t_k^j, t_{2k+1}^{j+1}, t_{k+1}^j, \dots, t_{n_j + m - 2}^j), & \text{if } n_j + m - 2 - \ell_2 < k < n_{j+1} - n_j, \\ (t_{k+1-\ell_1}^j, t_{k+2-\ell_1}^j, \dots, t_k^j, t_{2k+1}^{j+1}, t_{k+1}^j, \dots, t_{k-1+\ell_2}^j, t_{k+\ell_2}^j) & \text{otherwise.} \end{cases}$$

With these settings the above algorithms can be applied as before, using the modification for multiple knots described in Sect 2.

5.2. Periodic spline wavelets. Many problems deal with periodic functions. Our approach can easily be modified to define periodic spline wavelets. A P -periodic spline space can be defined if the knots satisfy the periodicity condition

$$t_{k+n} = t_k + P, \quad k \in \mathbb{Z}$$

for some $n \in \mathbb{N}$. Then the periodic spline space can be defined as

$$\begin{aligned} S_{m,\mathcal{T}}^P &:= \left\{ s \in S_{m,\mathcal{T}} : s(t) = s(t + P), t \in \mathbb{R} \right\} \\ &= \left\{ \sum_{k \in \mathbb{Z}} c_k N_{m,k}^{\mathcal{T}} : c_k = c_{k+n} \right\} = \text{span} \left\{ N_{m,k}^{\mathcal{T},P} : k = 1, \dots, n \right\} \end{aligned}$$

with the periodic B-splines

$$N_{m,k}^P := N_{m,k}^{\mathcal{T},P} := \sum_{\ell \in \mathbb{Z}} N_{m,k}^{\mathcal{T}}(\cdot + \ell P) = \sum_{\ell \in \mathbb{Z}} N_{m,k+\ell n}^{\mathcal{T}}.$$

To define wavelets we introduce again nested knot sets $\mathcal{T}^j = (t_k^j)_{k \in \mathbb{Z}}$, $j \in \mathbb{N}_0$, satisfying $t_k^j + P = t_{k+n_j}^j$, $k \in \mathbb{Z}$, $n_j = \lceil n_{j+1}/2 \rceil$, and $t_k^j = t_{2k}^{j+1}$, $k = 0, \dots, n_j - 1$. The corresponding periodic spline wavelets are then defined as

$$\psi_{j,k}^P := \sum_{\ell \in \mathbb{Z}} \psi_k^j(\cdot + \ell P) = \sum_{\ell \in \mathbb{Z}} \psi_{k+\ell(n_{j+1}-n_j)}^j.$$

Now the algorithms introduced above can be immediately adapted for periodic splines, using the fact that any P -periodic spline is uniquely determined by the vectors $(t_k)_{k=0}^{n-1}$ and $(c_k)_{k=0}^{n-1}$. All of the above algorithms can be applied using $t_k = t_{\kappa_1(k)} + \kappa_2(k)P$ for spline knots and $c_k = c_{\kappa_1(k)}$ for coefficients, where the mapping $\kappa : \mathbb{Z} \rightarrow \{0, \dots, n-1\} \times \mathbb{Z}$ is uniquely determined by $k = \kappa_1(k) + n \kappa_2(k)$.

5.3. Further generalizations. Following the ideas of [4, 5] and §3–4 one can consider further generalization. However, this leads to a more complex notation, while the principal ideas stay the same. Since the goal of this publication is to present an efficient and plain implementation with easily maintainable code we did not consider all possible generalizations, but only those which may give an advantage in our target applications. However, since the focus may change with other problems under consideration, we will give here some suggestions on possible generalized settings, where the ideas from our approach can still be applied.

Choice of Ξ_k^j . Apparently we could replace ℓ_1 and ℓ_2 in (3.3) by any $\ell_1(k)$ and $\ell_2(k)$, as long as $\ell_1(k) + \ell_2(k) = m + \tilde{m}$. Such a modification has been done for the boundary wavelets on the interval. However, the current choice was made to get some symmetry, which is often of advantage.

More general settings for the knot sequence Ξ_k^j are possible as long as it contains t_k^{j+1} and $m + \tilde{m}$ knots from \mathcal{T}^j . The algorithms would follow the same principle, but the support size would increase and the implementation would become more involved with no obvious advantage.

Choice of grids \mathcal{T}^j . As long as $\mathcal{T}^j \subset \mathcal{T}^{j+1}$, any sequence of knot sets can be used. For each new knot $t_k^{j+1} \notin \mathcal{T}^j$ a wavelet is defined (3.2), where Ξ_k^j contains t_k^{j+1} and $m + \tilde{m}$ additional knots from \mathcal{T}^j (which should be close to t_k^{j+1}). The algorithms would work analogously. However, one has to deal with the more complex setting, while the handling of the grids would require extra memory and computation time.

6. Wavelets for grid adaptation. An interesting property of wavelet is that they permit an efficient adaptive approximation using the best n -term approximation. That is, the function is approximated by a linear combination of n adaptively chosen wavelets. For a stable wavelet basis the wavelets with the largest expansion coefficients yield the best approximation. The approximation is optimal for functions from Besov spaces (see e.g. [26]). The same approximation power is obtained with free knot splines, i.e., B-spline representations with adaptively chosen knots. This is apparent, since any spline wavelet representation is a particular spline with adaptive knots (but not vice versa).

A simple rule of thumb is that an adaptive spline scheme is of benefit for functions with isolated singularities (e.g. discontinuities of the function or its (higher

order) derivatives, sharp transients). By a local refinement, i.e., additional wavelets or additional spline knots in the vicinity of such isolated singularities, one can achieve an accurate approximation with a relative small number of degrees of freedom. Going for the optimum means to determine the free knot spline of *best approximation*, which minimizes the approximation error for a given number of spline knots. Often it is not possible to find this optimal approximation at reasonable cost such that one looks instead for an *almost* best approximation, where the error has at least the same order of magnitude as the best approximation.

In this section we show how our spline wavelets can be used to generate an adaptive grid of spline knots. To achieve this goal we will use the fact that the wavelet ψ_k^J corresponds by definition with the knot t_{2k+1}^{j+1} .

6.1. Coarsening. In practice one can obtain an efficient n -term approximation as follows. We start from a sufficiently accurate spline approximation, i.e., an expansion in terms of scaling functions φ_k^J with sufficiently large J , which can be obtained e.g. by interpolation or quasi-interpolation. Next the fast decomposition algorithm is used to compute the multiscale wavelet expansion (4.13). From this expansion the terms with small coefficients are removed (thresholding), which may reduce the size of the expansion essentially, while only a small error is introduced.

Let us consider the simple case that $J = 1$. That is an application of the decomposition algorithm yields

$$s_1 = s_0 + \sum_k d_k^0 \psi_k^0. \quad (6.1)$$

Thresholding means that one replaces s_1 by

$$\tilde{s}_1 = s_0 + \sum_{k: |d_k^0| \geq \varepsilon} d_k^0 \psi_k^0. \quad (6.2)$$

Subtracting (6.2) from (6.1) one obtains

$$\tilde{s}_1 = s_1 - \sum_{k: |d_k^1| < \varepsilon} d_k^1 \psi_k^1.$$

Obviously \tilde{s}_1 can be computed by a modified version of the decomposition algorithm. In particular, Step 1(b)iv and 2(b) (with correspondingly modified Θ_k) in Algorithm 1 are only performed if $|d_k^1| < \varepsilon$. The result is \tilde{s}_1 in the B-spline expansion over the coarsened grid

$$\tilde{\mathcal{T}}_1 := \mathcal{T}^1 \setminus \{t_{2k+1}^1 : |d_k^1| < \varepsilon\}.$$

The above method can be applied successively to \tilde{s}_1 in order to obtain further coarsened representations \tilde{s}_j on $\tilde{\mathcal{T}}_j$.

In this process the spline grid will be adapted according to the approximated function. Starting from an approximation with required accuracy on a uniform or nonuniform grid unnecessary knots will be removed. This will mainly happen in areas, where the function is smooth such that it can be approximated by a polynomial of degree $< m$. In localities where the function is less smooth (e.g. isolated singularities or fast transients) few or no knots will be removed to keep the error under control.

The error can be controlled as follows. The normalization factor α_k^0 in (3.2) is chosen such that the coefficients $b_{k,\ell}$ in (4.8) satisfy

$$\max_{\ell} |b_{k,\ell}| = 1. \quad (6.3)$$

In practice this is done by computing $b_{k,\ell}$ and γ_k for $\alpha_k^0 = 1$, and divide these coefficients by $\max_\ell |b_{k,\ell}|$ afterwards. Then we have

$$|\psi_k^0(t)| < \max_\ell |b_{k,\ell}| = 1.$$

Due to their compact support (see §3), all but $m + \tilde{m} - 1$ wavelets vanish for any $t \in \mathbb{R}$. Therefore

$$|\tilde{s}_1(t) - s_1(t)| = \left| \sum_{k: |d_k^1| < \varepsilon} d_k^1 \psi_k^1(t) \right| \leq \varepsilon \sum_k |\psi_k^1(t)| \leq (m + \tilde{m} - 1)\varepsilon$$

and

$$|\tilde{s}_j(t) - s_1(t)| \leq (m + \tilde{m} - 1)j\varepsilon.$$

6.2. Refinement. It is not always possible to obtain an approximation on a very fine grid, and if possible it may be too expensive. In particular, for the approximative solution of operator equations the reason of an adaptive grid is to reduce the computational cost for the (often computationally expensive) solver, by reducing the number of degrees of freedom. That is, the number of degrees of freedom has to be kept as small as possible.

Let us assume we are able to compute a spline approximation of a function f for any grid in finite time, which increases at least linearly with the grid size. Namely, we denote by $A_{\mathcal{T}}(f)$ an approximation method yielding a spline approximation $f_{\mathcal{T}} = A_{\mathcal{T}}(f) \in S_{m,\mathcal{T}}$ of f on the grid $\mathcal{T} = (t_k)_{k=0}^n$. Typical examples for $A_{\mathcal{T}}(f)$ are collocation or Galerkin solvers for a differential equation.

Our approach is now to start with a coarse initial grid \mathcal{T}^0 and determine a first approximation $f_0 := A_{\mathcal{T}^0}(f)$. Now we want to use information contained in f_0 to generate a new improved grid. Performing a wavelet decomposition (Algo. 1) we obtain

$$f_0 = \tilde{f} + \sum_k d_k \psi_k^0,$$

Obviously, a large $|d_k|$ implies a large approximation error of the coarse scale approximation $\tilde{f} = \sum_k c_k \varphi_k^0$ in the support of ψ_k^0 , i.e., in a neighborhood of t_{2k+1} . Moreover, a large wavelet coefficient may also indicate a large approximation error of f_0 near t_{2k+1} . This assumption is justified for a large family of functions, e.g. solutions of typical differential or integral equations. Our goal is to improve the approximation locally in regions with a large local approximation error by refining the grid locally in these regions. Namely, we insert

$$n_k := \left\lceil |d_k| \frac{\alpha}{\max_\ell |d_\ell|} \right\rceil$$

equidistant knots into the intervals (t_{2k}, t_{2k+1}) and (t_{2k+1}, t_{2k+2}) , $k = 0, \dots, n-1$, which yields the refined grid \mathcal{T}^1 . Obviously knots are only inserted if $|d_k|$ is not below the threshold $\varepsilon := \frac{\max_\ell |d_\ell|}{\alpha}$ and the number of inserted knots grows with $|d_k|$. The factor $\alpha > 1$ controls the refinement rate. Note that the coarse scale approximation $\tilde{f} = \sum_k c_k \varphi_k^0$ is not needed here, i.e., we can stop the decomposition after

the computation of the wavelet coefficient in the decomposition algorithm (Algo. 1, Step1(b)iii).

Now we determine the improved approximation $f_1 := A_{\mathcal{T}^1}(f)$. We cannot expect this approximation to be sufficiently accurate, but we have gained additional information for another wavelet refinement. Thus, we repeat refinements until we have gained the required accuracy, which results in the following algorithm.

ALGORITHM 3.

Wavelet based grid refinement

INPUTS: m spline order
 \tilde{m} number of vanishing moments for wavelets
 \mathcal{T}^0 initial spline knot sequence
 ε error tolerance

OUTPUTS: \mathcal{T}^i final spline knot sequence
 f_i spline approximation on \mathcal{T}^i

CODE:

1. $f_0 := A_{\mathcal{T}^0}(f)$
2. FOR $i = 1, 2, 3, \dots$
 - (a) Compute the wavelet coefficients d_k , $k = 0, \dots, n-1$, of f_{i-1}
 - (b) Determine \mathcal{T}^i by inserting $n_k := \left\lfloor |d_k| \frac{\alpha}{\max_\ell |d_\ell|} \right\rfloor$ new knots into $(t_{2k}^{i-1}, t_{2k+1}^{i-1})$ and $(t_{2k+1}^{i-1}, t_{2k+2}^{i-1})$ for $k = 0, \dots, n-1$,
 - (c) $f_i = A_{\mathcal{T}^i}(f)$
 - (d) IF $\|f_i - f_{i-1}\| < \varepsilon$ stop with solution f_i

The above algorithm is of particular interest, if the approximation method is based on an iterative method, e.g. Newton's method for a nonlinear problem. Then an initial guess and a stopping criterion is required for the iteration, i.e., the approximation method $A_{\mathcal{T}}(f)$ is replaced by $A_{\mathcal{T}}(f, f^*, \varepsilon)$, where f^* is the initial guess and ε a tolerance to stop the iteration. In the above algorithm step 2(c) is replaced by $f_i = A_{\mathcal{T}^i}(f, f_{i-1}, \varepsilon_i)$. That is we use the already known approximation f_{i-1} , where the spline representation for the new grid \mathcal{T}^i is determined by the Oslo algorithm. Thus, for larger i we have an excellent initial guess, such that only a few Newton steps (often only one) are sufficient. Furthermore, for small i , where many (possibly damped) Newton steps may be necessary due to a bad initial guess, the grid is much smaller such that the cost for one step can be neglected. Thus, with a suitable refinement rate α , the overall computational cost may be comparable to the cost of few Newton steps on the final grid.

The stopping criterion in step 2(d) is based on the assumption that the approximation is essentially improved by the refinement. This assumption is justified if α is chosen sufficiently large to ensure a non negligible growth of the grid. Then it can be expected that the approximation error is in the range of ε when the algorithm stops. Due to the refinement we expect the grid to be adapted to the solution, i.e., coarser at smooth parts of f and finer at non smooth parts. However, a final coarsening can sometimes improve the efficiency of the approximation by essentially reducing the grid size while introducing only an insignificant additional error.

7. The application of wavelet based grid adaptation in circuit simulation. The described methods have been implemented as a C++ library, which can

be used in suitable applications. Here, we present results from an adaptive circuit simulation method. Details about the method can be found in [7–10] so that we will give only a short introduction here. By a Modified Nodal Analysis [28, 31] (which is based on Kirchoff’s laws and device models) one obtains the circuit equations

$$\frac{d}{dt}q(x(t)) + \underbrace{i(x(t)) + s(t)}_{g(x(t),t)} = 0, \quad (7.1)$$

where $x : \mathbb{R} \rightarrow \mathbb{R}^N$ denotes the unknown voltages and currents, $q : \mathbb{R}^N \rightarrow \mathbb{R}^N$ contains charges and fluxes from capacities and inductivities, $i : \mathbb{R}^N \rightarrow \mathbb{R}^N$ describes static contributions from resistors, diodes, transistors, etc., while $s : \mathbb{R} \rightarrow \mathbb{R}^N$ contains independent sources. Typically the Jacobian of $q(x)$ is not invertible, i.e., (7.1) is a system of differential algebraic equations (DAE).

7.1. Periodic steady state computation. To determine the periodic steady state of the circuit, we have to solve a periodic boundary problem, i.e., the solution of (7.1) has to satisfy $x(t) = x(t + P)$.²

We discretize (7.1) by a spline-based Petrov-Galerkin method. That is, the unknown solution is expanded as a P -periodic spline $x = \sum_{k=1}^n c_k N_{m,k}^P$ for unknown coefficients $c_k \in \mathbb{R}^N$. Integrating (7.4) over a suitable chosen set of n subintervals $[\tau_{\ell-1}, \tau_{\ell}]$ yields the system of $n \times N$ nonlinear equations

$$F_{\ell}(c_1, \dots, c_n) := \omega(\tau_{\ell}) \left(q(x(\tau_{\ell})) - q(x(\tau_{\ell-1})) \right) + \int_{\tau_{\ell-1}}^{\tau_{\ell}} g_k(x(t), t) dt, \quad \ell = 1, \dots, n. \quad (7.2)$$

This system can be solved numerically by applying Newton’s method.

Due to their support properties the use of the B-spline expansion (with free knots) has some advantages compared with the use of a wavelet expansion (cf. [11, 18, 24]). First one has to evaluate $x(t)$ many times. For a B-spline expansion this is much more efficient compared to a wavelet expansion. Furthermore, the Jacobian of $(F_{\ell}(c_1, \dots, c_n))_{\ell=1, \dots, n}$ is much sparser for the B-spline expansion. Since the computation of the Jacobian and solving the linear system require most of the computation time this sparsity is essential for the efficiency of the algorithm.

However, it remains open how the spline knots have to be chosen for an efficient computation. This is in particular important if the circuit exhibits digital like behavior, i.e., the solution switches between a finite number of states with sharp transients. Then a grid adapted to the signal waveforms in the circuit will yield a sparser representation, which makes the simulation much more efficient. Thus, the grid refinement described in Algo. 3 is used to determine an adaptive grid, where $x_i = A_{\mathcal{T}^i}(x, x_{i-1}, \varepsilon_i)$ denotes the Newton’s method for (7.2).

For the described circuit simulation problem the advantages of our new algorithms are fully exploited. Most of the computation time is consumed by the (sparse) linear solver and by the evaluation of q and g with their Jacobians, which are usually expensive due to the complex models for semiconductor devices. The remaining computations including the wavelet transforms take only $\approx 1\%$ of the simulation time. Thus, the little extra computation time, which may be needed compared to classical wavelet transform, fully pays off due to smaller linear systems and fewer function evaluations.

²An approach for initial value problems (Transient Analysis) using splines on the interval is described in [9, 10].

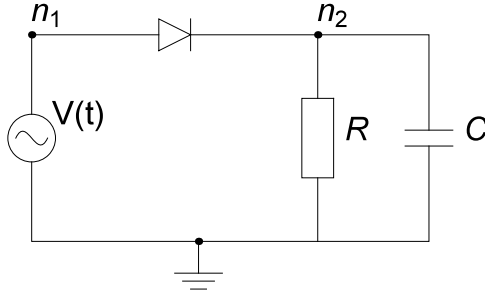


FIG. 1. Diode Rectifier

Diode rectifier. As a first example we show simulation results for a diode rectifier (Fig. 1). This is a very simple circuit, but it permits to demonstrate in illustrative manner how the refinement algorithm works. The diode becomes conductive if the branch voltage exceeds a threshold of roughly 0.5V. Thus, the output voltage at n_2 jumps up, if the sinusoidal input voltage an n_1 exceeds a certain value and goes down slowly due to the discharging of the capacitor. The refinement algorithm was used with a refinement rate $\alpha = 2.5$, which is large enough to increase the grid size fast enough to stop the algorithms after a few step, while a larger α would result in a larger grid, which makes the final steps of the algorithm to time consuming. The stopping tolerance was chosen as $\varepsilon = 0.02$ so that the algorithm stops when no visual improvements can be seen anymore. It can be observed in Fig. 2 that the grid is in particular refined at the sharp transient of the output signal near $25\mu s$, leading to an improved representation of that signal.

Finally the spline expansion is coarsened to reduce the size of the expansion, using a threshold of 0.006 over several iterations. Obviously the coarsening makes the approximation much more efficient. This is due to the fact the wavelet based local error estimator yields only a guess of the refinement location. Although, this is a relative good guess, it is still a guess, and the solution can be essentially improved by throwing out unnecessary spline knots after the simulation.

7.2. Multirate simulation. Although spline wavelet based circuit simulation yields reliable results at reasonable cost for initial value or periodic steady state problems, its most interesting application is in multirate envelope simulation. Details about multirate circuit simulation can be found in [7, 8, 13, 32, 39, 40]. Here we follow the presentation in [7, 8].

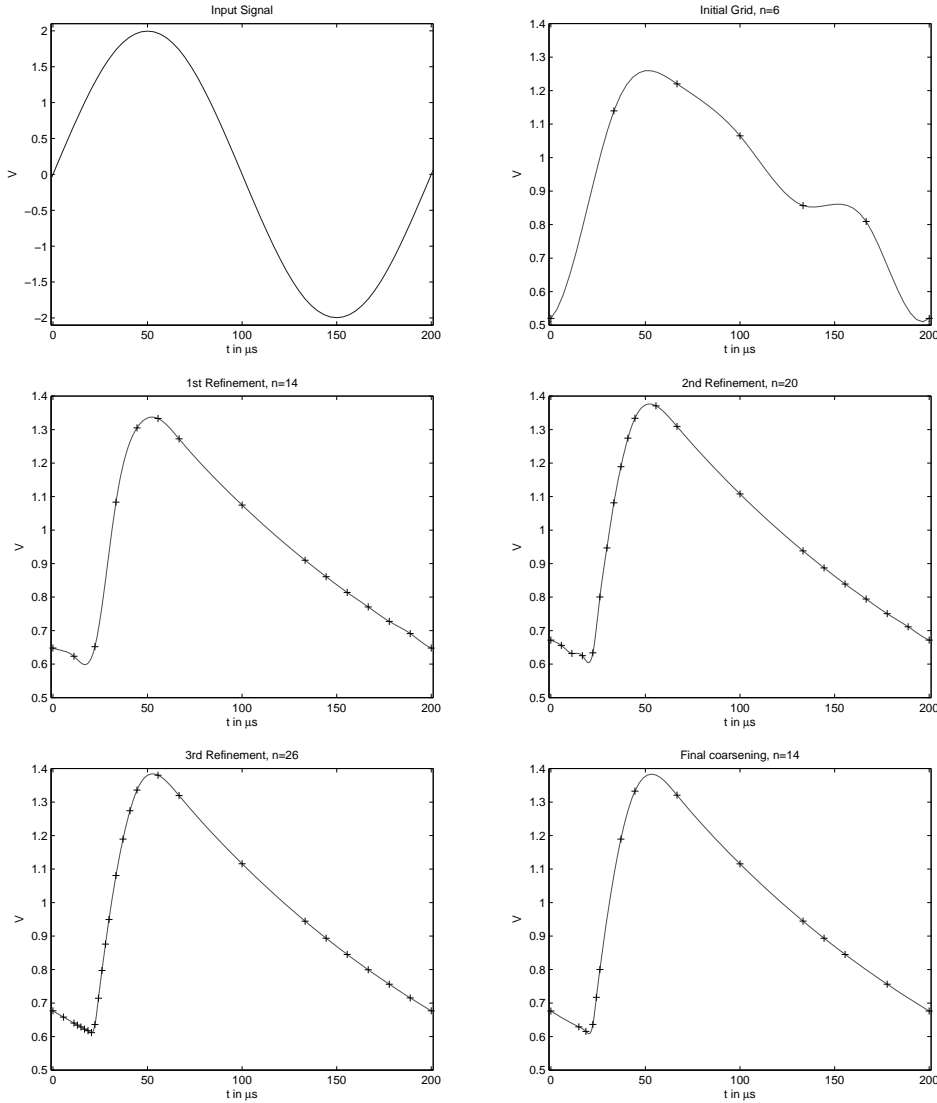
In multirate problems, the solution can be described as a fast oscillating carrier signal modulated by a slow changing envelope signal, as it occurs usually in Radio Frequency (RF) problems. To separate the different scales the ordinary DAE's (7.1) is replaced by a system of partial differential algebraic equations (PDAE's) of the form

$$\frac{\partial}{\partial \tau} q(\hat{x}(\tau, t)) + \omega(\tau) \frac{\partial}{\partial t} q(\hat{x}(\tau, t)) + g(\hat{x}(\tau, t)) = \hat{s}(\tau, t) \quad (7.3)$$

under the conditions

$$\hat{x}(0, t) = X_0(t), \quad \hat{x}(\tau, t) = \hat{x}(\tau, t + P).$$

The solution of (7.1) is obtained as the solution of (7.3) along characteristic curves, i.e., $x(t) = \hat{x}(t, \Omega(t))$. For typical multirate signals the bivariate envelope solution

FIG. 2. *Simulation Results for Diode Rectifier*

$\hat{x}(\tau, t)$ is smooth such that it can be approximated much more efficiently than the original solution $x(t)$, since the limits of Nyquist's sampling theorem are avoided.

For the numerical solution we perform a semi-discretization with respect to τ (Rothe method), which is done by a multi-step method (namely Gear's BDF technique, see e.g. [29, 30]). By this approach we find for each time step τ_k , $k \in \mathbb{N}$, an approximation $X_k(t)$ of $\hat{x}(\tau_k, t)$, $\tau_{k+1} > \tau_k > \tau_0 = 0$, as solution of an ordinary DAE

$$\omega(\tau_k) \frac{d}{dt} q(x(t)) + g_k(x(t), t) = 0, \quad x(t) = x(t + P). \quad (7.4)$$

Here, $g_k(x, t)$ is determined by the used multi-step method and depends therefore on solutions X_ℓ , $\ell < k$, at previous time steps (see [7, 8] for details).

The periodic problem (7.4) is of the same structure as the original circuit equations

(7.1) and thus solved by the method described in §7.1. For typical multirate problems the solution $\hat{x}(\tau, t)$ is very smooth in τ . Thus, the solution X_{k-1} of the previous step can be expected to be a good approximation for X_k and therefore a good initial guess for the first Newton iteration (Step 1. in Algo. 3). But due to the grid refinements the size of the spline grid would increase for each time step τ_k . Therefore a wavelet based grid coarsening (§6.1) is applied to X_{k-1} , to get rid of unnecessary knots. Summing up, the *refinements* will provide the required accuracy, while the grid *coarsening* is responsible for the sparsity of the grid, which ensures the efficiency of the simulation.

One advantage of our method is that information from previous steps is used for grid generation and Newton's initial guess. This is a crucial difference to an earlier approach in [2], where the *uniform* wavelet decomposition of the solution of an initial value problem is used to generate an adaptive grid for a finite difference method on the periodic problem. Due to an excellent initial guess, Newton's method stops after a few iteration steps, often needing only one refinement with a moderate refinement rate $\alpha < 2$. This can be achieved with a properly tuned step size control for the BDF method, and a threshold for the coarsening, which is an order of magnitude below the required accuracy. In our algorithm we use a time step control, which uses a priori and a posteriori error estimates and simultaneously controls the number of Newton steps. The optimization of this time step control is the object of current research.

Phase Locked Loop (PLL). We have used the described method to simulate a Phase Locked Loop (PLL) containing 205 MOSFET Transistors, and $N = 112$ unknowns. This is a relatively complex circuit consisting of a voltage controlled oscillator (VCO), frequency dividers, a phase frequency detector (PFD), and a loop filter. For details we refer to [7, 8]. The input signal is a frequency modulated sinusoidal signal with center frequency 25kHz. The baseband signal is also sinusoidal with frequency 10Hz and frequency deviation 100Hz. Central components as frequency dividers and the PFD are digital circuitry so that many internal signals exhibit sharp transients. Thus, adaptive grid generation shall lead to improved performance. We have chosen $P = 40\mu s$ which corresponds to the center frequency. The factor $\omega(\tau_k)$ is chosen by a method described in [8] to get a smooth solution.

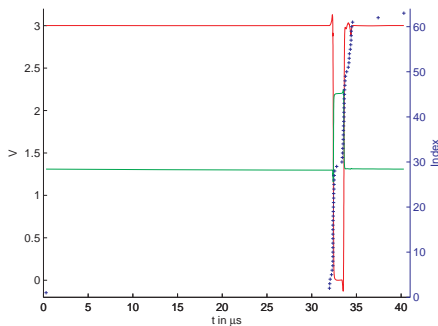


FIG. 3. Two simulated signals of the PLL and the corresponding spline knots t_k , where each + stands for a pair (t_k, k) .

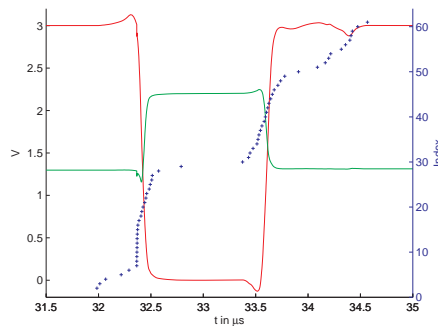


FIG. 4. Detail of Fig. 3.

Fig. 3 shows two components of the approximated solution X_{20} at $\tau_{20} = 72\mu s$ together with the corresponding spline grids. For each spline knot we have plotted the pair (t_k, k) , which gives a better picture of the grid in particular at locations where

the grid is locally dense. Together with the detail plot in Fig. 4 the example shows an excellent adaptation to the signal shapes, with high knot density at locations of sharp signal transients.

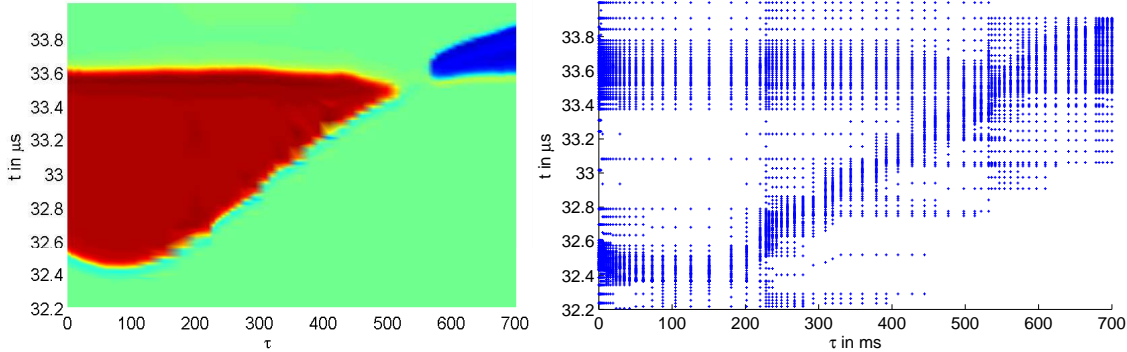


FIG. 5. Detail of the solution of the multirate simulation of a PLL (density plot) together with the discretization grid.

The grid development over several time steps τ_k is illustrated in Figure 5. One can see that the grid is refined at the location of sharp signal transients, while the coarsening successfully removes knots which are no longer needed in later time steps.

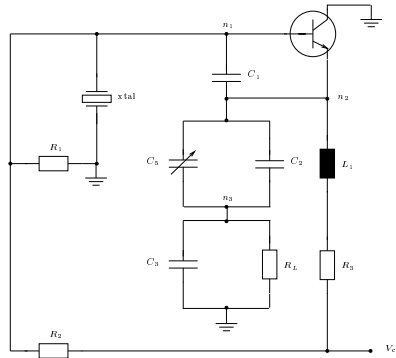


FIG. 6. 3MHz Colpitts quartz oscillator.

Colpitts Oscillator. Another example is the start up phase of a 3MHz Colpitts quartz crystal oscillator (see Fig. 6). With $N = 8$ this is a smaller circuit. More details can be found in [6], where also the problem of numerical damping is treated. For this problem we have chosen $P = 1$, so that $\omega(\tau_k)$ determined by the method from [8] will be close to $3 \cdot 10^6$, which corresponds to the oscillator frequency.

The transistor used as feedback amplifier introduces some nonlinear effects into the output signal (see Fig. 7), which result in a sharp edge near $t = 0.24\mu s$, which becomes apparent at the end of the start up phase at $\tau \approx 5ms$. Obviously the grid refinement can handle this emerging edge, and adapts even to a change of location for increasing τ .

REFERENCES

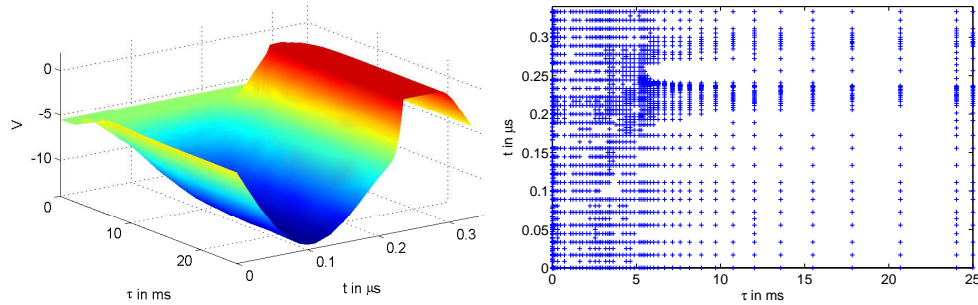


FIG. 7. Multi-rate solution for 3MHz Colpitts oscillator and the corresponding adaptive grid.

- [1] A. BARINKA, W. DAHMEN, AND R. SCHNEIDER, *Fast computation of adaptive wavelet expansions*, Numer. Math., 105 (2007), pp. 549–589.
- [2] A. BARTEL, S. KNORR, AND R. PULCH, *Wavelet-based adaptive grids for multirate partial differential-algebraic equations*, Appl. Numer. Math, 59 (2009), pp. 495–506.
- [3] G. BATTLE, *A block spin construction of ondelettes. part i: Lemarié functions*, Commun. Math. Phys., 110 (1987), pp. 601–615.
- [4] K. BITTNER, *Biorthogonal spline wavelets on the interval*, in Wavelets and Splines: Athens 2005, Guanrong Chen and Ming-Jun Lai, eds., Nashboro Press, Brentwood, TN, 2006, pp. 93–104.
- [5] ———, *On the stability of compactly supported biorthogonal spline wavelets*, in Approximation Theory XII: San Antonio 2007, Mike Neamtu and Larry Schumaker, eds., Nashboro Press, Brentwood, TN, 2008, pp. 38–49.
- [6] K. BITTNER AND H.-G. BRACHTENDORF, *Trigonometric splines for oscillator simulation*, in 22nd International Conference Radioelektronika, 2012, pp. 1–4.
- [7] ———, *Adaptive multi-rate wavelet method for circuit simulation*, Radioengineering, 23 (2014), pp. 300–307.
- [8] ———, *Optimal frequency sweep method in multi-rate circuit simulation*, COMPEL, 33 (2014), pp. 1189–1197.
- [9] K. BITTNER AND E. DAUTBEGOVIC, *Adaptive wavelet-based method for simulation of electronic circuits*, in Scientific Computing in Electrical Engineering 2010, Bastiaan Michiels and Jean-René Poirier, eds., Mathematics in Industry, Springer, Berlin Heidelberg, 2012, pp. 321 – 328.
- [10] ———, *Wavelets algorithm for circuit simulation*, in Progress in Industrial Mathematics at ECMI 2010, M. Günther, A. Bartel, M. Brunk, S. Schöps, and M. Striebel, eds., Mathematics in Industry, Springer, Berlin Heidelberg, 2012, pp. 5 – 11.
- [11] K. BITTNER AND K. URBAN, *Adaptive wavelet methods using semiorthogonal spline wavelets: Sparse evaluation of nonlinear functions*, Appl. Comput. Harmon. Anal., 24 (2008), pp. 94–119.
- [12] W. BOEHM, *Inserting new knots into a B-spline curve*, Computer-Aided Design, 12 (1980), pp. 199–201.
- [13] H. G. BRACHTENDORF, *Theorie und Analyse von autonomen und quasiperiodisch angeregten elektrischen Netzwerken. Eine algorithmisch orientierte Betrachtung*. Universität Bremen, 2001. Habilitationsschrift.
- [14] M. D. BUHMANN AND C. A. MICHELLI, *Spline prewavelets for non-uniform knots*, Numerische Mathematik, 61 (1992), pp. 455–475.
- [15] C. K. CHUI AND E. QUAQ, *Wavelets on a bounded interval*, in Numerical Methods in Approximation Theory, D. Braess and L. L. Schumaker, eds., vol. 9, Birkhäuser, Basel, 1992, pp. 53–75.
- [16] C. K. CHUI AND J. WANG, *A general framework of compactly supported splines and wavelets*, J. Approx. Theory, 71 (1992), pp. 54–68.
- [17] ———, *On compactly supported spline wavelets and a duality principle*, Trans. Amer. Math. Soc., 330 (1992), pp. 903–915.
- [18] A. COHEN, W. DAHMEN, AND R. DEVORE, *Sparse evaluation of compositions of functions using multiscale expansions*, SIAM J. Math. Anal., 35 (2003), pp. 279–303 (electronic).
- [19] A. COHEN, I. DAUBECHIES, AND J.-C. FEAUVEAU, *Biorthogonal bases of compactly supported wavelets*, Comm. Pure and Appl. Math., 45 (1992), pp. 485–560.

- [20] E. COHEN, T. LYCHE, AND R. RIESENFELD, *Discrete B-splines and subdivision techniques in computer aided geometric design and computer graphics*, Comp. Graphics and Image Proc., 14 (1980), pp. 87–111.
- [21] W. DAHMEN, A. KUNOTH, AND K. URBAN, *Biorthogonal spline-wavelets on the interval — stability and moment conditions*, Appl. Comp. Harm. Anal., 6 (1999), pp. 132–196.
- [22] W. DAHMEN AND C. A. MICCHELLI, *Banded matrices with banded inverses ii: Locally finite decomposition of spline spaces*, Constructive Approximation, 9 (1993), pp. 263–281.
- [23] W. DAHMEN AND R. SCHNEIDER, *Wavelets with complementary boundary conditions—function spaces on the cube*, Results Math., 34 (1998), pp. 255–293.
- [24] W. DAHMEN, R. SCHNEIDER, AND Y. XU, *Nonlinear functionals of wavelet expansions — adaptive reconstruction and fast evaluation*, Numer. Math., 86 (2000), pp. 49–101.
- [25] C. DE BOOR, *A Practical Guide to Splines*, Springer, New York, 1978.
- [26] R. A. DEVORE, *Nonlinear approximation*, Acta Numerica, 7 (1998), pp. 51–150.
- [27] M. ECK AND J. HADENFELD, *Knot removal for B-spline curves*, Comput. Aided Geom. Des., 12 (1995), pp. 259–282.
- [28] M. GÜNTHER, U. FELDMANN, AND J. TER MATEN, *Modelling and discretization of circuit problems*, in Numerical Analysis in Electromagnetics, Special Volume of Handbook of Numerical Analysis, W.H.A. Schilders and J. ter Maten, eds., vol. XIII, Elsevier Science BV, Amsterdam, 2005.
- [29] E. HAIRER, S.P. NØRSETT, AND G. WANNER, *Solving ordinary differential equations: Nonstiff problems*, Springer series in computational mathematics, Springer, 1993.
- [30] E. HAIRER AND G. WANNER, *Solving Ordinary Differential Equations II: Stiff and Differential-Algebraic Problems*, Springer Series in Computational Mathematics, Springer, 2010.
- [31] C. W. HO, A. E. RUEHLI, AND P. A. BRENNAN, *The modified nodal approach to network analysis*, IEEE Trans. Circuits and Systems, CAS-22 (1975), pp. 504–509.
- [32] S.H.M.J. HOUBEN, *Simulating multi-tone free-running oscillators with optimal sweep following*, in Scientific Computing in Electrical Engineering 2010, W.H.A. Schilders, E.J.W. ter Maten, and S.H.M.J. Houben, eds., Mathematics in Industry, Springer, Berlin, 2004, pp. 240 – 247.
- [33] R. KAZINNIK AND G. ELBER, *Orthogonal decomposition of non-uniform Bspline spaces using wavelets*, Computer Graphics forum, 16 (1997), pp. 27–38.
- [34] A. KUNOTH AND J. SAHNER, *Wavelets on manifolds: an optimized construction*, Math. Comp., 75 (2006), pp. 1319–1349 (electronic).
- [35] P.-G. LEMARIÉ, *Ondelettes à localisation exponentielles*, J. Math. Pures Appl., 67 (1988), pp. 227–236.
- [36] T. LYCHE AND K. MOERKEN, *Making the oslo algorithm more efficient*, SIAM J. Numer. Anal., 23 (1986), pp. 663–675.
- [37] T. LYCHE, K. MØRKEN, AND E. QUAK, *Theory and algorithms for non-uniform spline wavelets*, in Multivariate Approximation and Applications, N. Dyn, D. Leviatan, D. Levin, and A. Pinkus, eds., Cambridge University Press, 2001, pp. 152–187.
- [38] M. PRIMBS, *New stable biorthogonal spline-wavelets on the interval*, Result. Math., 57 (2010), pp. 121–162.
- [39] R. PULCH, *Initial-boundary value problems of warped MPDAEs including minimisation criteria*, Math. Comput. Simulat., 79 (2008), pp. 117–132.
- [40] ———, *Variational methods for solving warped multirate partial differential algebraic equations*, SIAM J. Scient. Computing, 31 (2008), pp. 1016–1034.
- [41] E. G. QUAK AND N. WEYRICH, *Decomposition and reconstruction algorithms for spline wavelets on a bounded interval*, Appl. Comp. Harm. Anal., 1 (1994), pp. 217–231.
- [42] L. L. SCHUMAKER, *Spline Functions: Basic Theory*, Wiley, New York, 1981.